in Macaoay, Suzanne and Montgomery, William., Environmental Geology of the Highlands, 23rd Annual Meeting of the Geological Association of New Jersey, Ramapo College of New Jersey, p. 26-45.

Hydrogeological framework of Middle Proterozoic granite and gneiss from borehole geophysical surveys at two ground-water pollution sites, Morris County, NJ.

Gregory C. Herman, NJ Geological Survey

INTRODUCTION

The New Jersey Geological Survey (NJGS) collected borehole geophysical data in a set of 6-inch-diameter deep bedrock wells drilled into Middle Proterozoic granite and gneiss in Morris County, New Jersey. The data were collected at two ground-water pollution sites in 2002 and 2004 to identify and characterize the subsurface geology that controls the storage and movement of ground water and associated volatile organic compounds (VOCs) resulting from commercial manufacturing and waste disposal activities. Both sites are underlain by hornblende granite (Drake and others, 1996) and are about 3 miles apart along the structural strike (Fig. 1). Data were collected in one well at the first site (Site 1) and 5 wells at the second (Site 2). The depth of investigation for the geophysical investigations ranged from 17 to 511 ft below land surface (bls). Optical televiewer (OPTV), fluid temperature and fluid electrical resistivity or conductivity data were used to establish the hydrogeological framework. Heat-pulse flowmeter (HPFM) data were collected in 3 wells at Site 2 to locate water-bearing zones (WBZs) and to characterize borehole cross flows under natural conditions.

HYDROGEOLOGICAL INTERPRETATION

Borehole data were collected at Site 1 (Fig. 1) in December 2002 in an abandoned water-supply well located within an industrial center. The well lies within an extensive contaminant plume having VOC concentration levels exceeding NJ Dept of Environmental Protection maximum-contaminant-level standards (Gallagher and Volkert, 1990). The well is open to bedrock between 17 and 230 ft bls (Fig. 2). Well logs at Site 2 (Figs. 3 to 5) were collected from October to December 2004 in a set of test wells drilled to develop a public supply for a proposed housing development. The development is located immediately northeast and adjacent to an old landfill. VOC contaminants were detected in water from many of the test wells following a June 2004 sampling event at concentrations of as much as 218 parts-per-billion (Fig. 3). The 5 wells chosen for analyses were based on their depths, areal distribution, and reported contaminant levels. The wells logged at Site 2 were open to bedrock at depths ranging from 200 to 511 ft bls (Figs. 4 and 5).

Analyses of bedrock structures using OPTV records

The orientations of bedrock structures interpreted from the OPTV records were calculated using software supplied by the instrument manufacturer. Details of the OPTV instrument design and methods of deployment are covered in Herman (2005). Figure 6 shows how OPTV records represent borehole geometry with respect to traces of planar structures seen on the borehole walls. A dip-value (1^o to 90^o)/dip-azimuth (0^o to 359^o)

convention is used for specifying structural orientation of planar features unless otherwise noted.

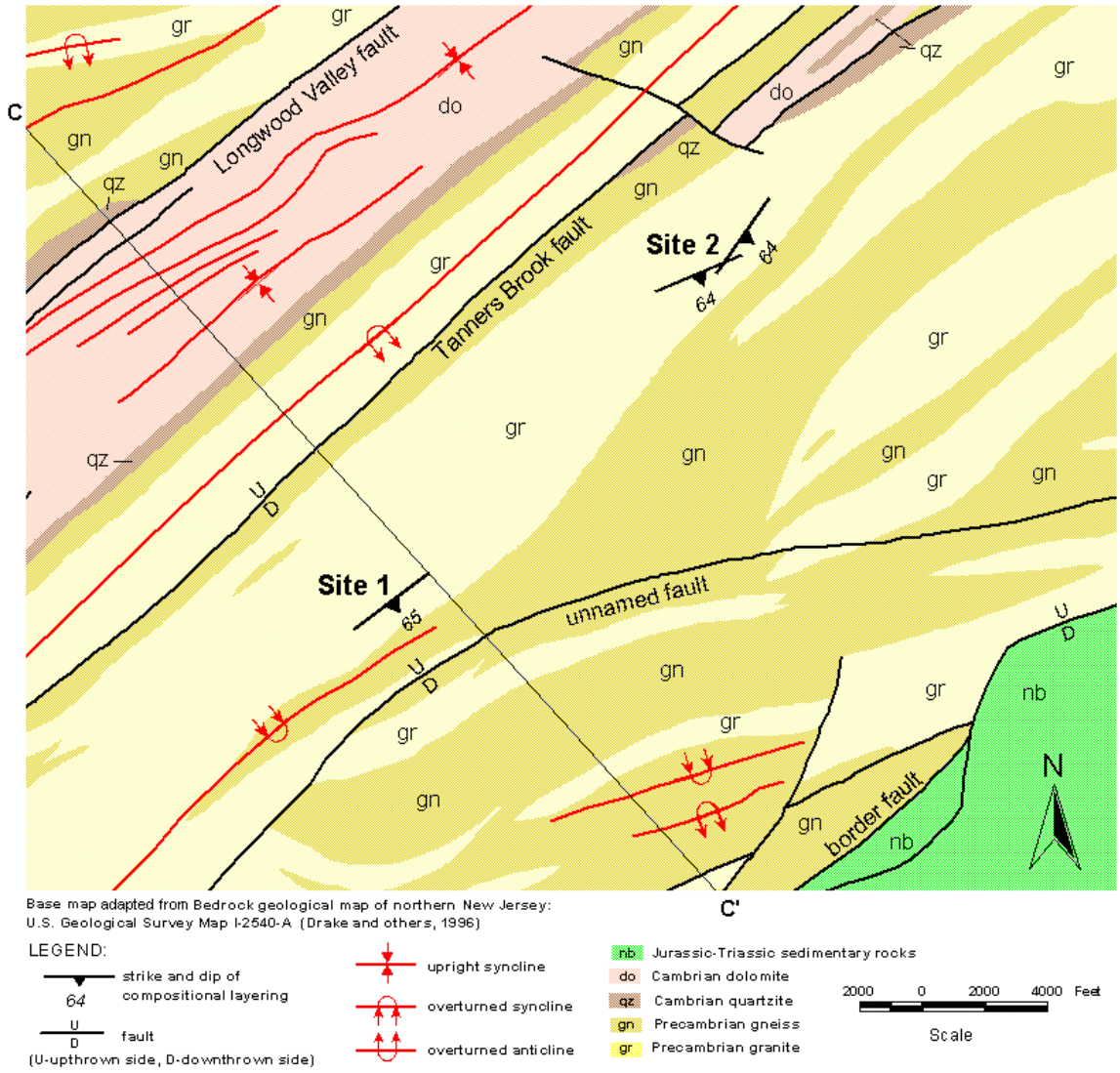

Figure 1.Generalized bedrock geology in the vicinity of two ground-water pollution sites in Morris County, New Jersey. Cross-section trace C-C' from Drake and others (1996).

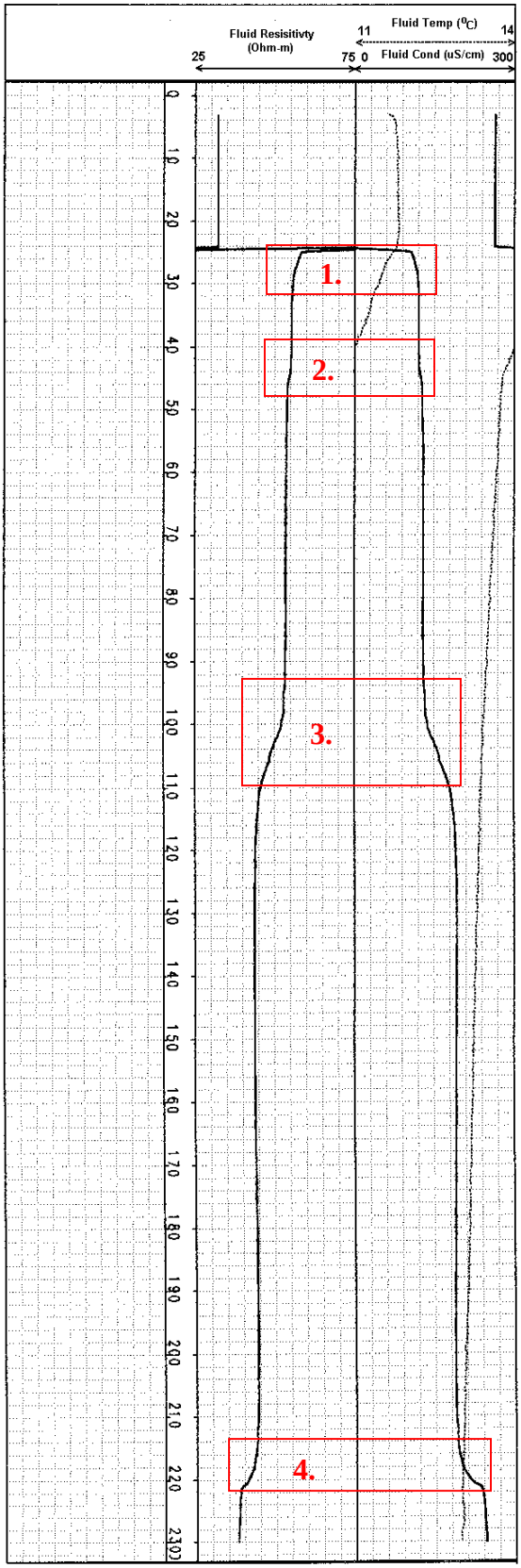

Figure 2. Fluid temperature, electrical resistivity and conductivity logs for the well at Site 1. Fluid temperature and electrical resistivity and conductivity anomalies are boxed and numbered. Anomalies 1 and 2 correspond to conductive structures shown in figure 13. Anomalies 3 and 4 correspond to conductive structures shown in figure 14. Figure 12 only shows conductive fractures over the lower part of interval 3. Other conductive, altered, gently- to moderately dipping fractures in the 93- to 110-ft interval are not shown.

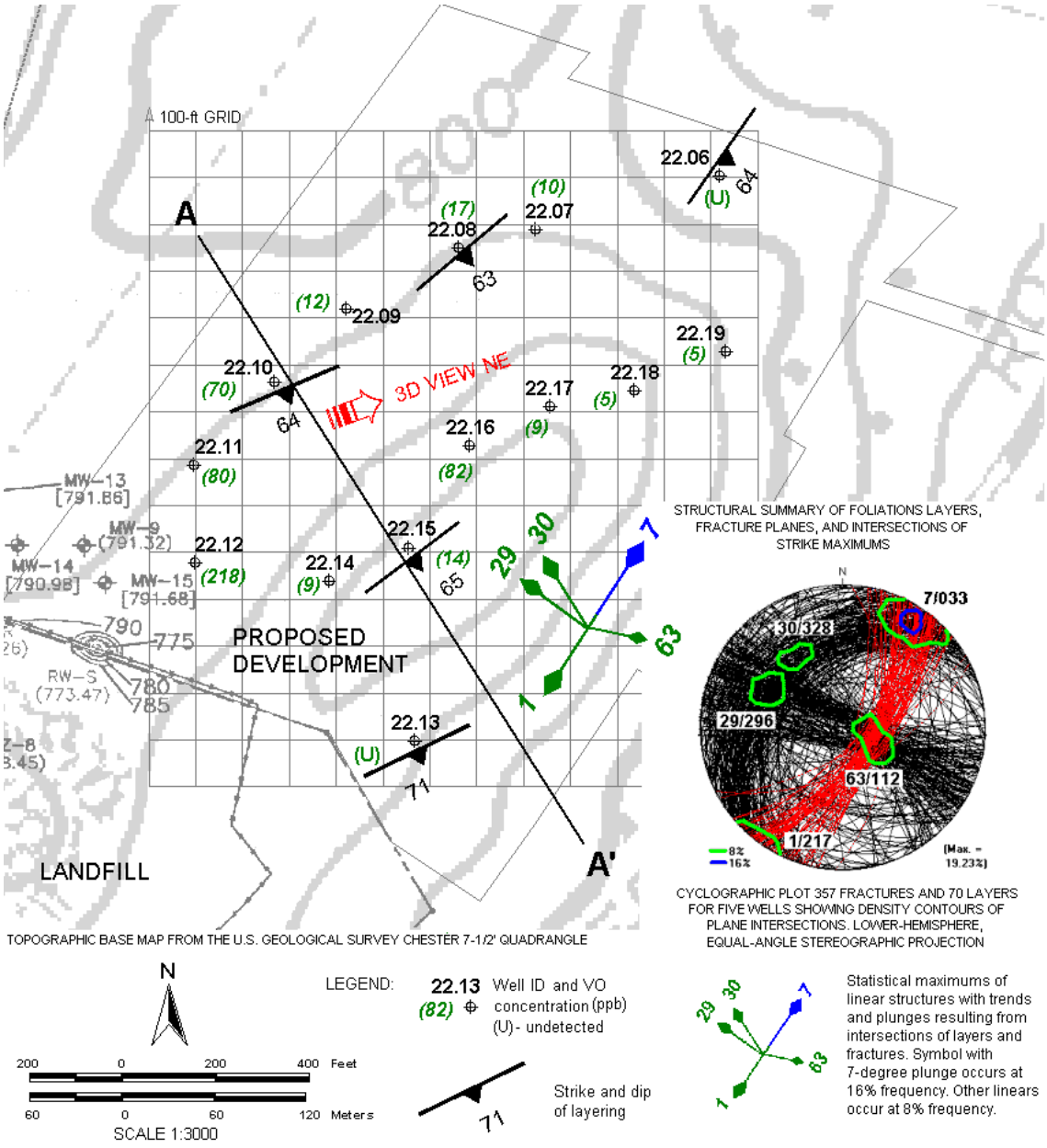

Figure 3. Site 2 map showing the location of test wells, contaminant concentration levels from the June 2004 sampling event, and structural summary of structural planes and plane intersections interpreted from OPTV records.

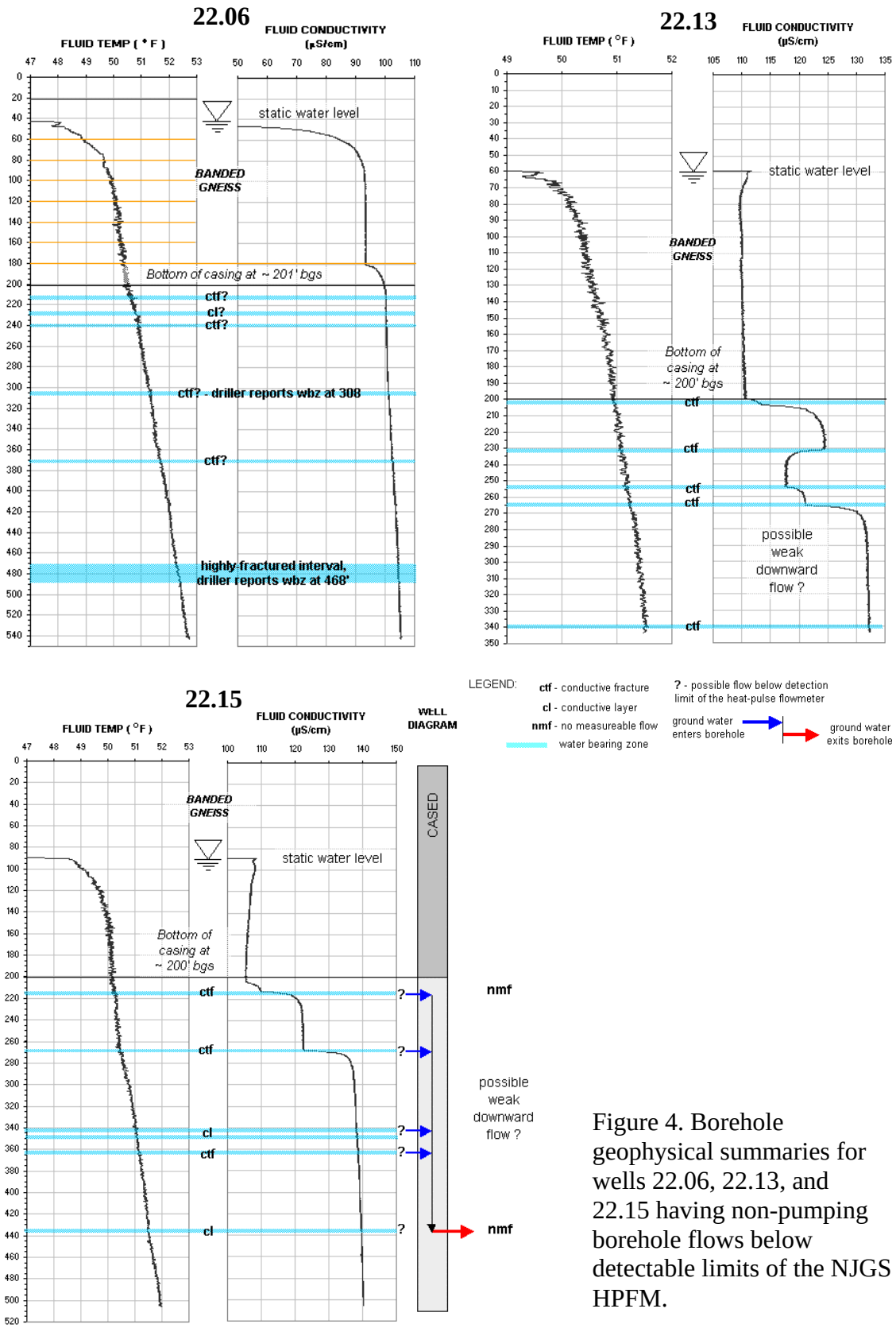

Figure 4. Borehole geophysical summaries for wells 22.06, 22.13, and 22.15 having non-pumping borehole flows below detectable limits of the NJGS HPFM.

22.08

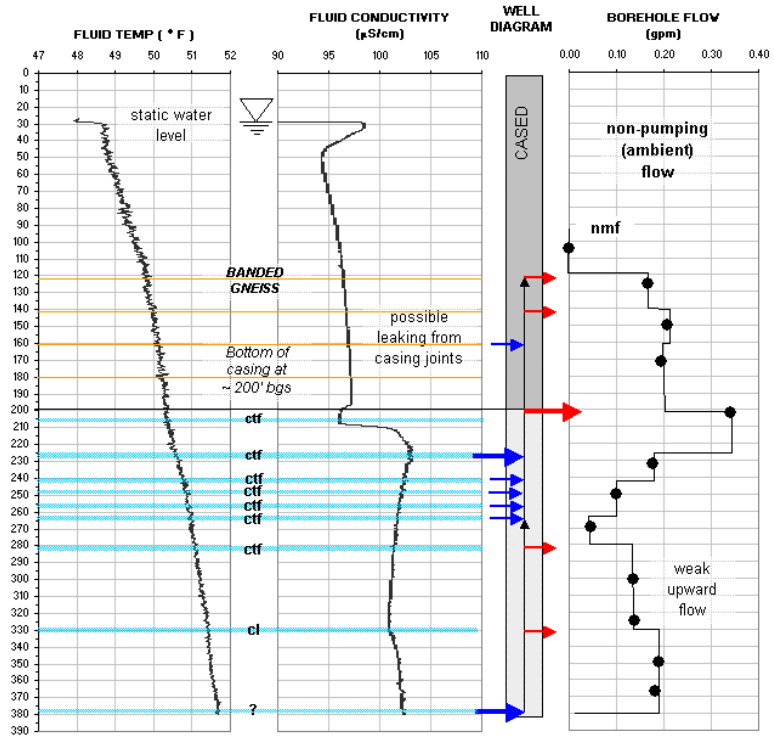

22.10

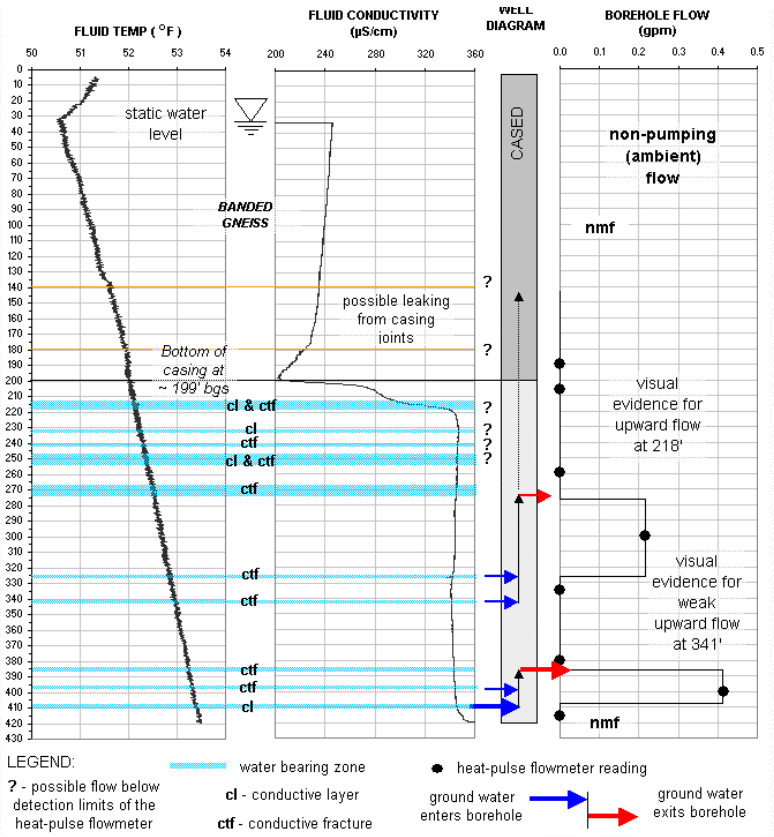

Figure 5. Borehole geophysical summaries for wells 22.08 and 22.10 having non-pumping upward flows measured with the NJGS HPFM

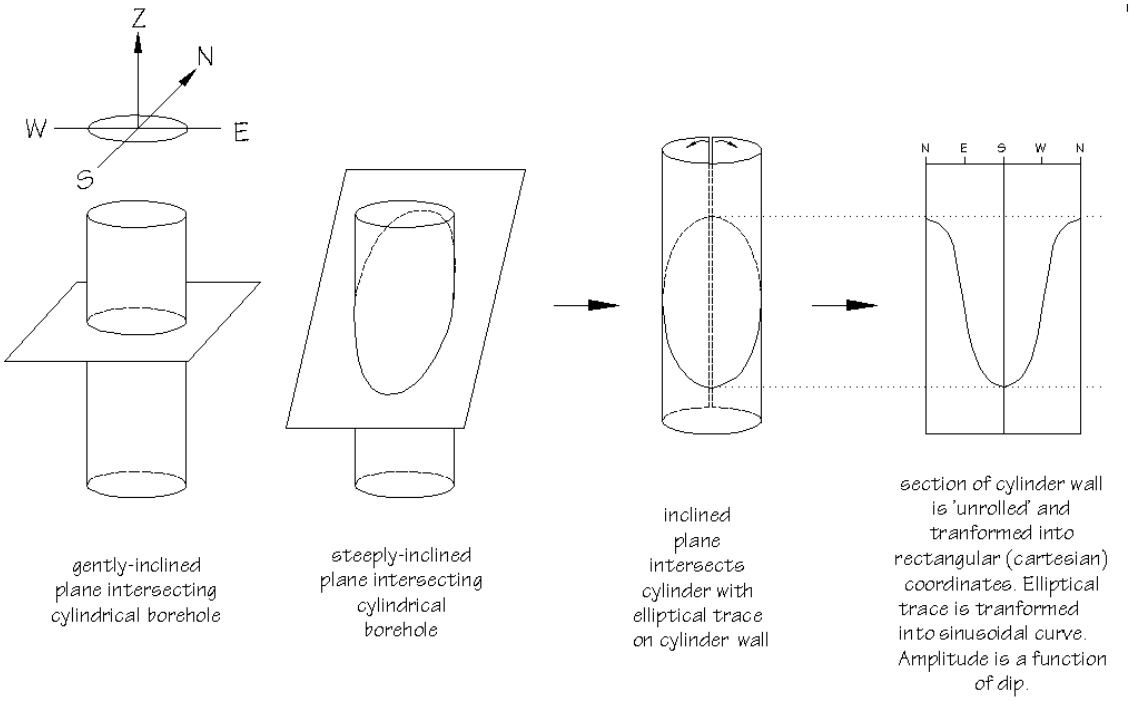

Figure 6. Structural diagrams summarizing the orientations of bedrock features interpreted from OPTV logs

Three primary types of planar structures were identified and measured (Fig. 7):

1) Compositional layering – Alternating dark-to-light lithologic layering or banding corresponding to granitic or gneissoid foliation. Dark layers are probably amphibole (hornblende) rich whereas light layers are probably composed mostly of quartz and feldspar (Volkert, 1989).

2) Fractures – Brittle, planar discontinuities but no visible shear offset of any other bedrock features cut by the fracture. Fractures were noted as mineralized wherever visible accumulations (~> 0.05 in. thick) of secondary minerals were visible in the fracture plane.

3) Shear fractures – Fractures that show shear offset of any other planar features cut by the fracture. Where visible accumulations of secondary minerals occur in the shear plane, these were noted.

The structural analysis relied on selective sampling of imaged borehole features. Individual layers and fractures were measured in 5-meter (~16 ft) stacked intervals. Fractures commonly cluster in sets with individual fractures arranged in stepped, parallel (en echelon) alignment (Fig. 8). Measured features are believed to represent numerous, closely spaced structures within the sample interval. Multiple measurements were taken of a particular feature within a sample interval where the strike or dip differed from a similar, previously measured feature by more than 5^{o}.

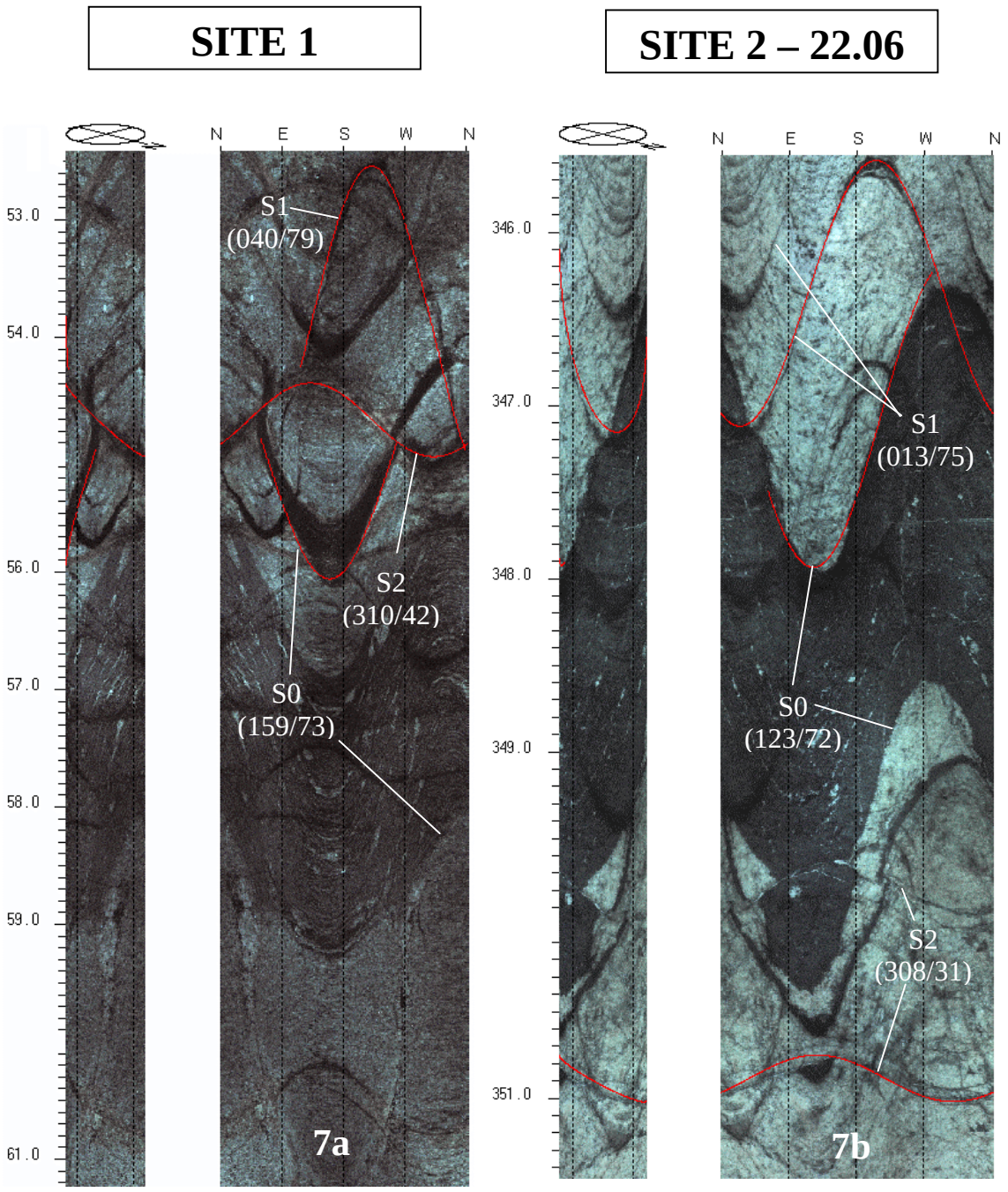

Figure 7. Representative OPTV records showing structural relationships common to both sites. Compositional layering (S0) is locally offset by steeply dipping cross fractures (S1) having normal dip-slip shear. Late-stage, gentle-to moderately dipping mineralized fractures also show localized shearing and offset of both S0 and S1 planes.

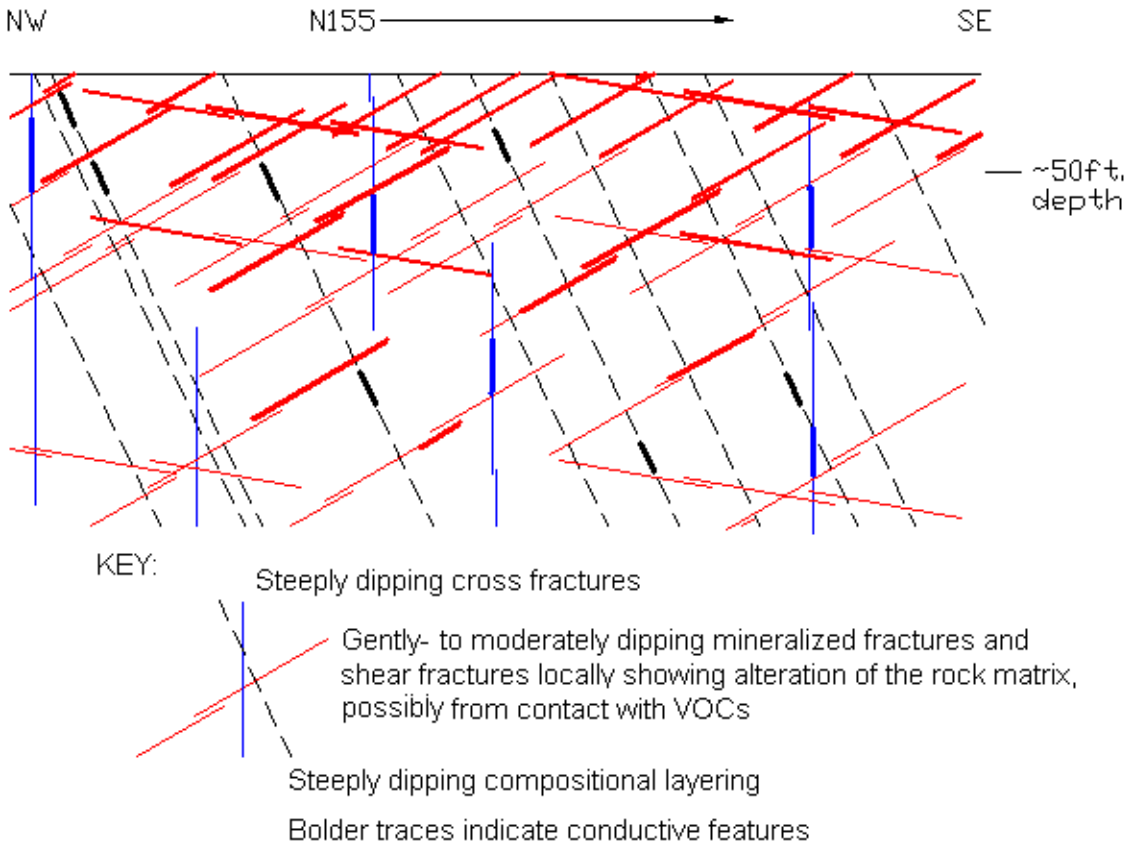

Figure 8. Schematic profile of the hydrogeologic framework of fractured bedrock at Sites 1 and 2. Bolder lines indicate structural planes that are locally conductive based on the fluid temperature and electrical conductivity/resistivity logs, the HPFM analyses, and alteration of bedrock close to fracture walls seen in the OPTV records (see text for further explanation). The most abundant conductive structures are mineralized fractures and shear planes dipping gently-to-moderately northwest. Effective secondary porosity in the bedrock results from the interaction of all of the different planar structures.

Structural orientations of lithologic layers and fractures interpreted from OPTV records are summarized in figure 9. The mean orientation of compositional layers and of fractures was determined using stereographic-projection diagrams. All measured fractures were combined for this analysis. The mean orientation of layering at Site 1 (65/156 = strike and dip N66^{o}E/65SE^{o}) agrees closely with the strike and dip of granite foliation measured in outcrop about 3000 ft to the southwest, about N65^{o}E/66SE^{o} (Volkert, 1989). The mean strike of layering at Site 2 (N32^{o}E) is rotated about 30^{o} counterclockwise relative to Site 1, but the mean dip of layering at both sites is about the same, 65^{o} to 66^{o} SE. Layers and fractures at both of these sites exhibit similar geometry and interrelationships. For example, both sites have primary sets of mineralized fractures and shear planes dipping northwest at gentle angles (1^{o} to 39^{o}) to moderate (40^{o} to 59^{o}) ones (Figs. 7 to 9). Shear fractures commonly cut and offset layering and other steeply-dipping (60^{o} to 90^{o}) fractures with a reverse dip-slip sense of shear (Figs. 7 and 10). Subordinate mineralized sets of fractures dip gently- to moderately southeast, and steeply dipping cross fractures

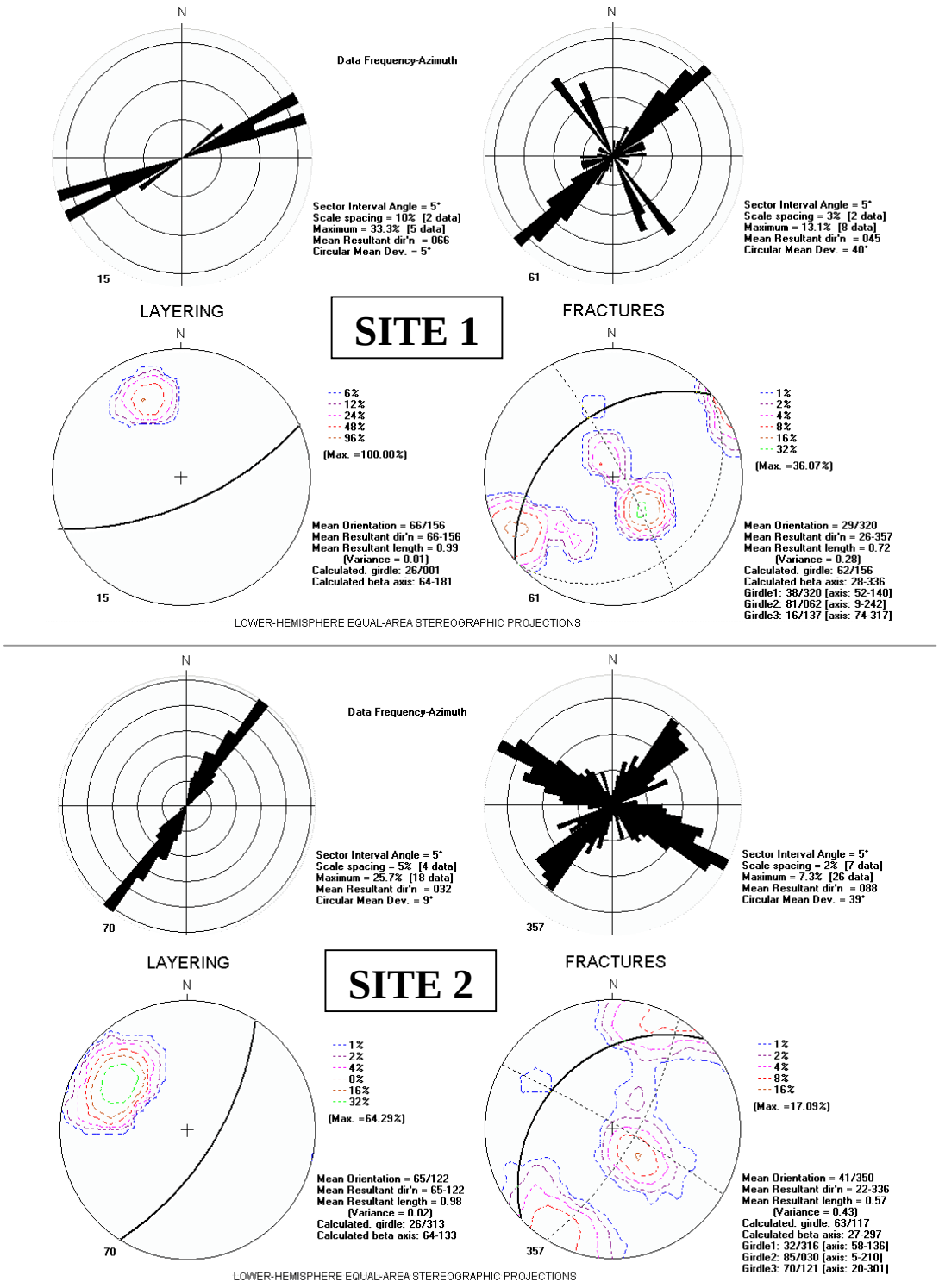

Figure 9. Diagrams summarizing the orientation of bedrock structures interpreted from OPTV logs for Site 1 (top) and Site 2 (bottom).). The mean orientation of layering and the primary fracture set are represented as bold, solid lines following the traces of great circles. Two subordinate sets of fracture planes at each site are identified using dashed lines following traces of great circles.

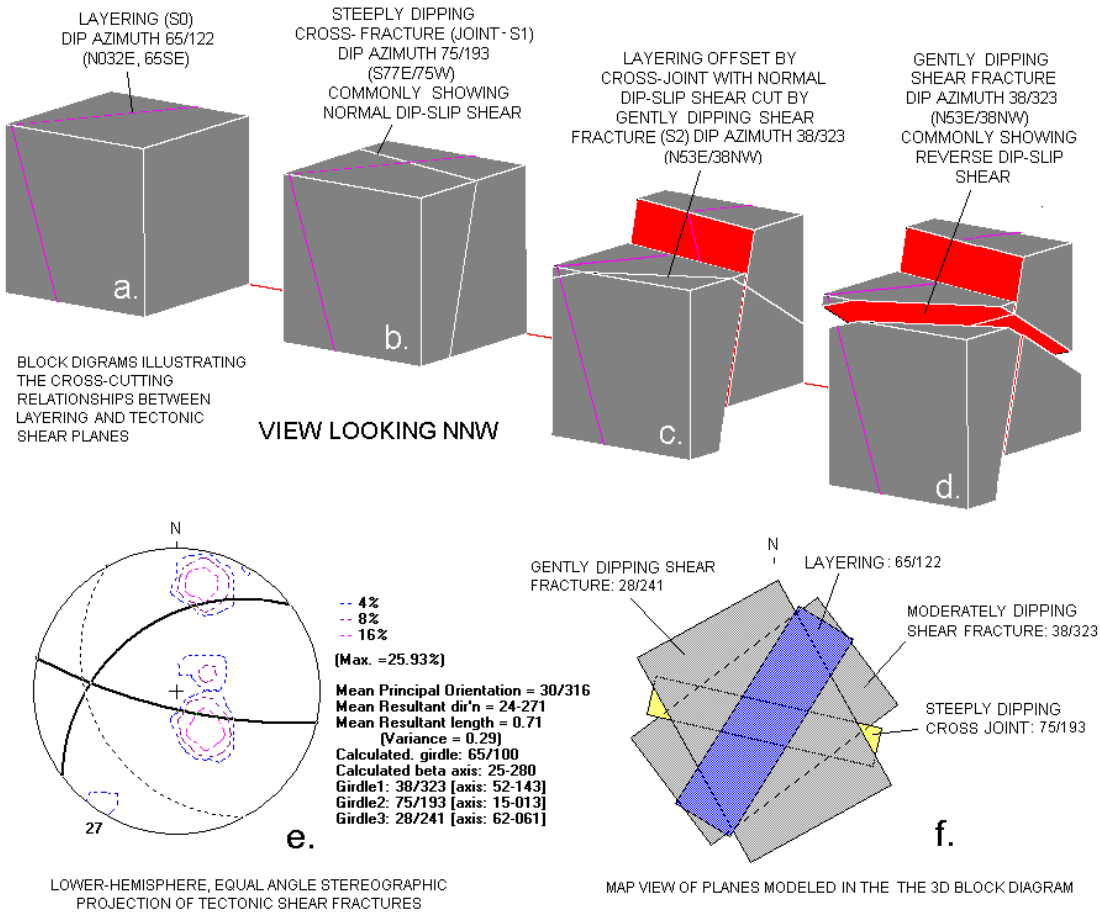

Figure 10. Structural diagrams illustrating the geometric relationship between layering and shear planes observed in the OPTV data at Site 2.

(or cross-joints) strike at complimentary angles to layering (Figs. 7 to 9). Cross fractures typically have dark, secondary minerals in the fracture plane, offset layering with a normal dip-slip sense of shear (Figs. 7 and 10), and display the same counterclockwise rotation of strike between sites as for layering (Fig. 9). These crosscutting relationships provide a relative sense of timing of structural development. Layering is the primary (S0) structural plane that is cut and locally offset by cross-strike extension fractures (S1). Both S0 and S1 structures are themselves cut and locally offset by gently-to-moderately-dipping fractures and shear planes (S2) respectively (Figs. 7 and 10).

Subsurface S2 fractures imaged with the OPTV are measured in outcrop throughout the New Jersey Highlands where they are commonly filled with dark-green, chlorite and/or chloritoid secondary minerals (Fig. 11). Map and profile plots of these fractures measured through the northeast highlands along a cross-strike traverse near Route 23 shows that these fractures also commonly dip northwestward (Fig. 12). Their origin probably stems from internal shearing strains associated with the emplacement of basement-cored, stacked fault slices in the region (Herman and others, 1997).

Figure 11. Example of outcropping, chlorite-filled shear fractures in Middle Proterozoic basement of the New Jersey Highlands, US Geological Survey Newfoundland 7-1/2’ quadrangle. Spaced sets of anastomosing shear fractures oriented ~N75E/25NW cut and offset foliation in pyroxene granite. Lens cap for a 35-mm camera shown for scale in figure 11a. Mechanical pencil shown for scale in figure 11b.

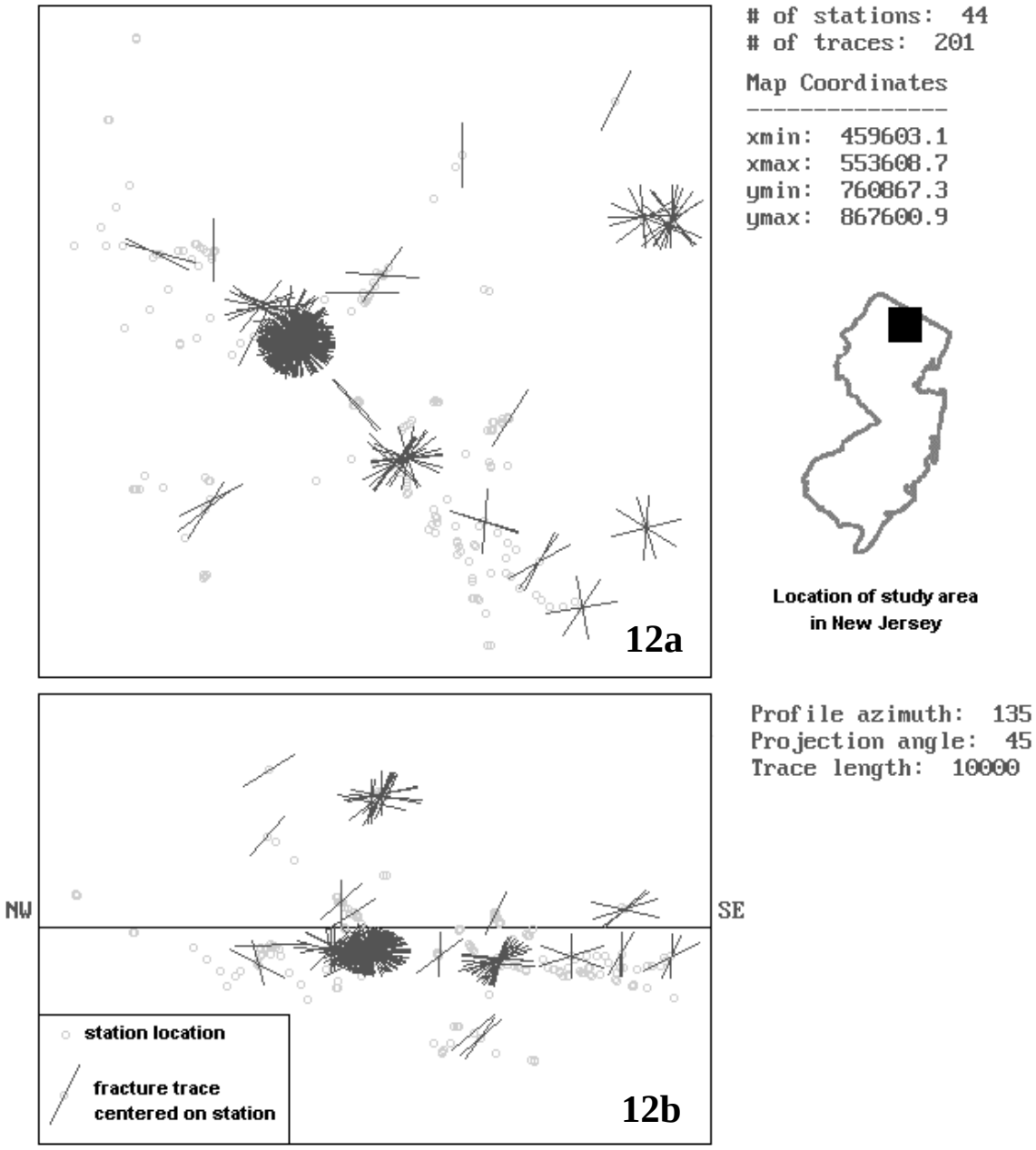

Figure 12. Map (12a) and profile projection (12b) of 201 chlorite- and epidote-filled shear fractures measured in outcrop along a northwest (NW) to southeast (SE) traverse through the New Jersey Highlands in 1985-86.

Identification and interpretation of hydraulically-conductive features and WBZs

Layering and fractures are noted as conductive (hydraulically) where they exhibit visible secondary porosity and correlate at depth to measured changes in the properties of the borehole fluids, or show other signs of ground water transmission. Changes in fluid properties include fluid-temperature and/or electrical resistivity/conductivity anomalies (Figs. 2, 4, and 5), and/or measured differences in borehole flows as determined with a HPFM (Fig. 5). Other visible signs of fracture conductivity include dark staining of the rock matrix close to a fracture (Figs. 13b, 14a and 15a), or points where fractures intersect layers or other fractures (Fig. 16a). Staining of the country rock as much as an inch from the fracture walls is probably an indication of ground-water contamination along mineralized fracture planes. Bedrock in uncontaminated wells and along nonconductive fractures shows no apparent staining along correlative fracture sets (Figs.7b, 14b and 15b). Staining may stem from chemical alteration of iron-rich minerals, such as chlorite, that fill fractures and shear planes. Although the process chemistry is unclear, a series of chemical reactions may involve the oxidation of iron and reductive dechlorination of VOCs in aqueous media (EnviroMetal Technologies, Inc., 1998).

Site 1

Fluid temperature and fluid electrical resistivity anomalies in the well logs at Site 1 indicate at least four potential WBZs (Fig. 2). The shallowest zone is near the static-water level where the bedrock is highly broken from 24 to 30 ft bls (Fig. 13a). A second zone at shallow depths of 44 to 46 ft and coincides with gently dipping fractures showing chemical alteration of fracture walls (Fig. 13b). A third zone at an intermediate depth from 98 to 110 ft bls also corresponds with conductive, moderately-to-gently-dipping fractures (Fig. 14a). The deepest zone occurs at 218 to 222 ft and coincides with secondary porosity developed along a layer-parallel fracture at a depth of 220 ft (Fig. 14b). Altered fracture sets are most abundant in the shallow subsurface at depths down to about 50 ft, where fluid temperatures show many small fluctuations (Figs. 2 and 8).

Site 2

Geophysical data in the wells at Site 2 show many WBZs resulting from all three types of structures, at all logged depths (Figs. 4 and 5). However, WBZs at conductive fractures outnumber those from compositional layering at about a 3:1 ratio. Most of the conductive fractures are S2 fractures that dip gently- to moderately northwest. The HPFM analyses show that borehole cross flows in some wells range from about 4 gpm to less than 0.5 gpm under natural (non-pumping) conditions (Fig. 5). The NJGS flow meter has been shown to be about 80 percent accurate in measuring upward-directed fluid flow at rates of about 0.7 to 25.0 gpm in standard, 6-inch bedrock wells (Herman, 2006). Low-flow rates below 0.5 gpm are more qualitative and rely on delayed heat-pulse arrival times, the geometric form of fluid-temperature and electrical anomalies, and visual evidence for the direction of flow from OPTV records (Fig. 15b, 341-ft depth).

Wells marked by the highest recorded contaminant levels are in the valley (Fig. 3) and display upward-directed flows (Fig. 5). Upward-directed cross flows stem mostly from inflows along northwest dipping S2 fractures. Wells exhibiting upward-directed flows are probably recharged at higher topographic elevations to the east (Fig. 3) under

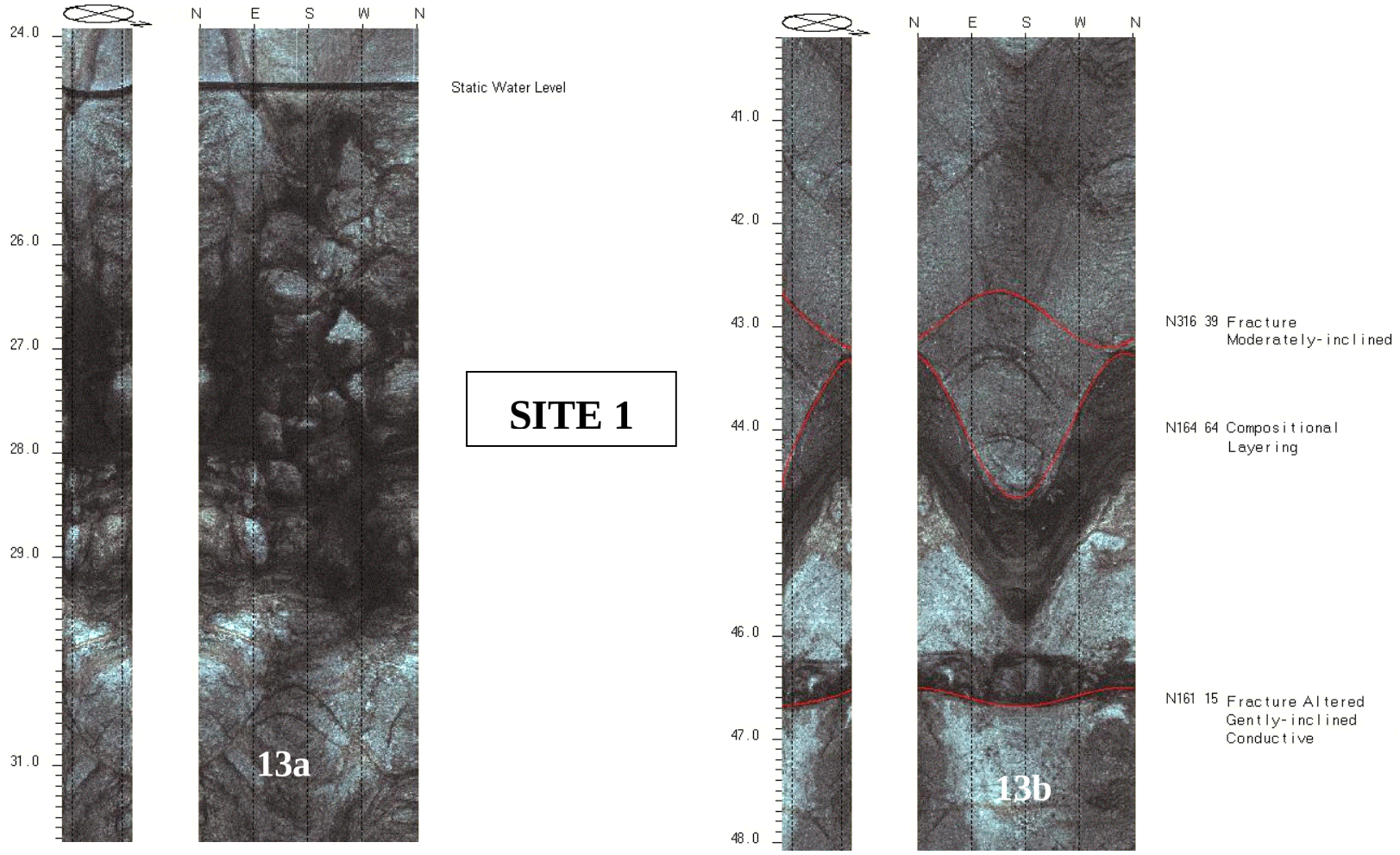

Figure 13. OPTV records of the two, uppermost water bearing zones in the well at Site 1. Locations of the zones correspond to fluid temperature and electrical resistivity/conductivity anomalies noted in figure 1.

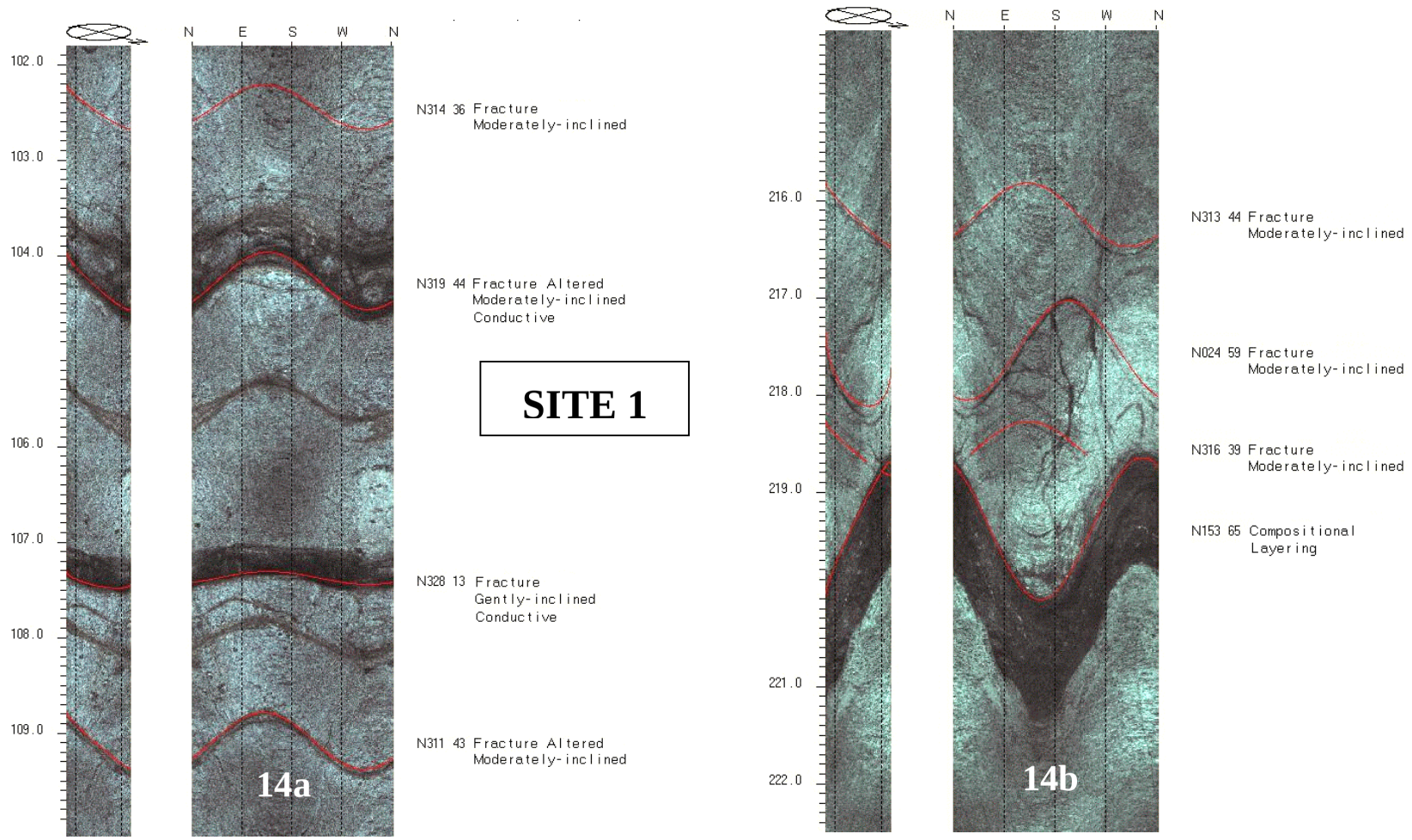

Figure 14. OPTV records of the lowermost WBZs in the Site 1 well. Locations of the zones correspond to fluid temperature and electrical resistivity/conductivity anomalies noted in figure 1. Conductive, moderately dipping fractures from ~ 93 to 99 ft depth show staining of the rock matrix adjacent to the fracture planes.

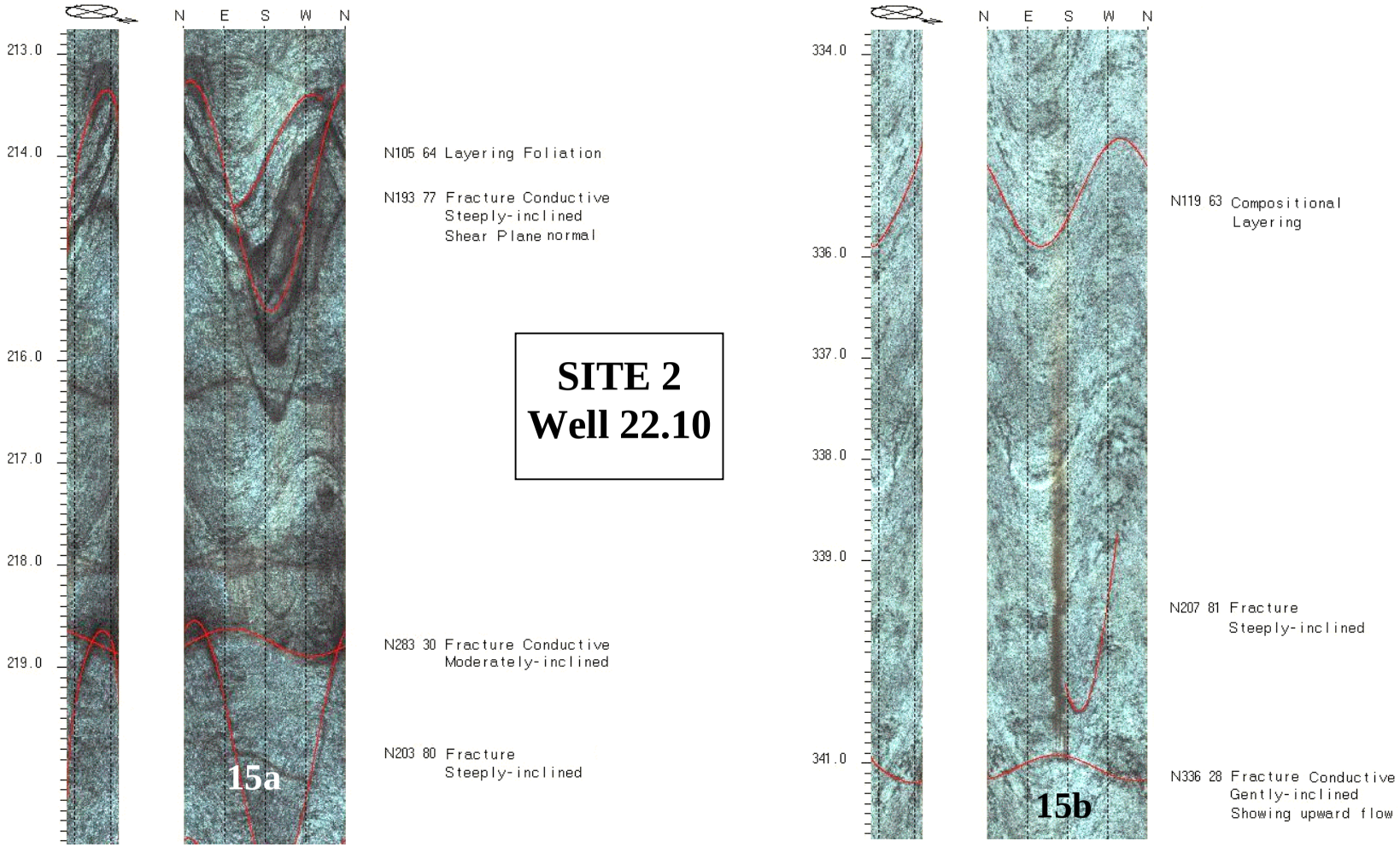

Figure 15. OPTV records of conductive structures in Site 2 well 22.10. Locations of the zones correspond to fluid temperature and electrical resistivity/conductivity anomalies noted in figure 5. Conductive, gently-dipping fracture at 341' shows visual evidence of upward cross flow in the well where rust-colored stain emanates from the conductive fracture.

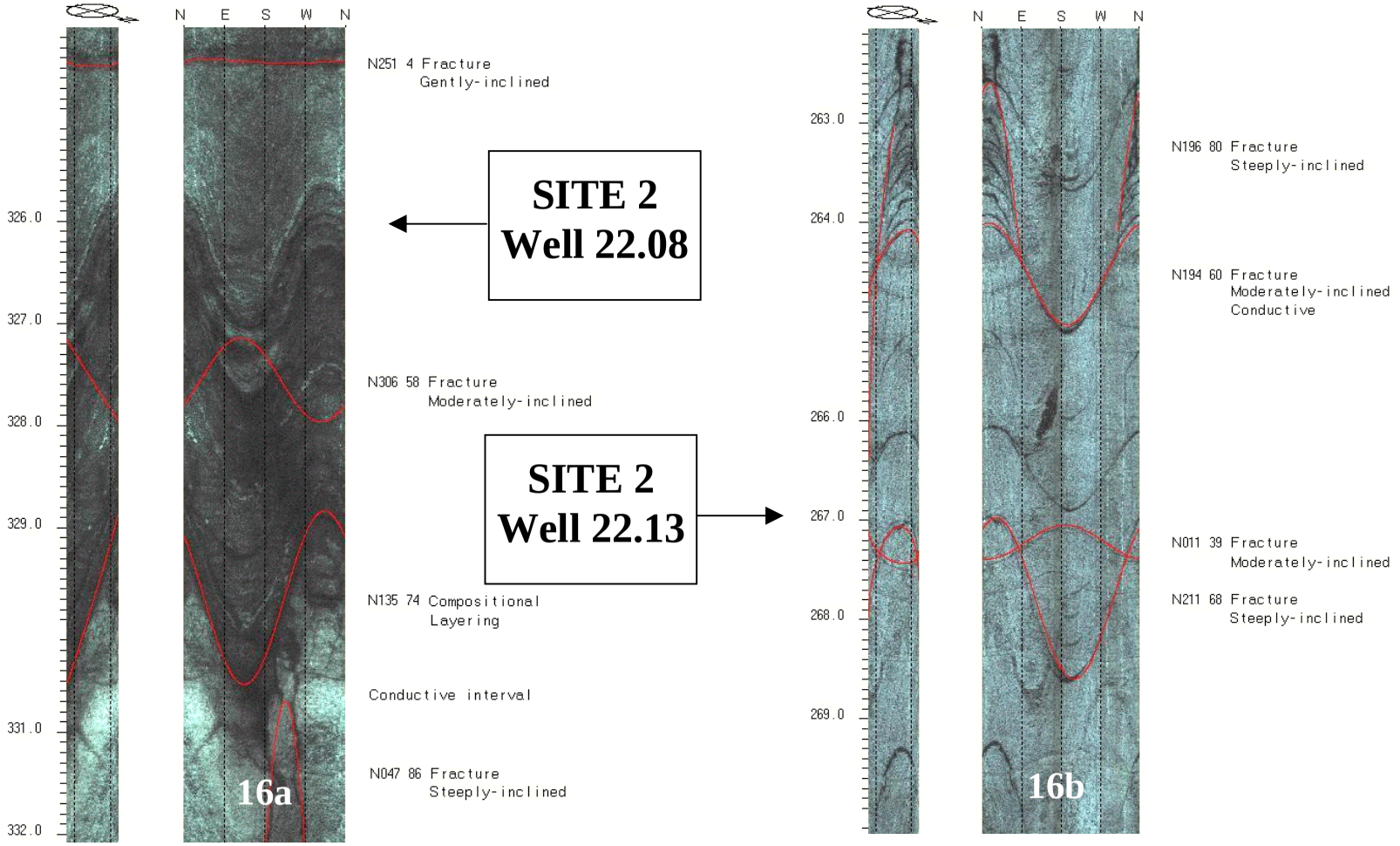

Figure 16. OPTV records of conductive structures in Site 2, wells 22.08 and 22.13. Locations of the zones correspond to fluid temperature and electrical resistivity/conductivity anomalies noted in figures 4 and 5.

semiconfined conditions. These wells provide a conduit for vertical cross flows and cross contamination of the aquifer under natural conditions. Wells situated toward the ridge crests probably harbor weak downward flows that lie below the detection limit of the HPFM (fig. 4). Fluid-temperature and fluid electrical conductivity anomalies in the cased parts of wells 22.06 and 22.08 indicate local cross flows in some cased intervals, probably attributable to water leaks at threaded pipe unions (figs. 4 and 5). A measurable cross flow was found in the cased part of well 22.08 (Fig. 5). HPFM measurements in well 22.08 also showed temporal variations in flow rate during data sampling. This suggests local well interference and transient water-table fluctuations in the area, probably from intermittent pumping of nearby domestic wells located on the flanks of the northeast-trending ridge extending through the proposed development.

Fracture alteration and staining are found at the deepest intervals imaged with the OPTV but are the densest at intermediate depths in wells 22.10 and 22.08 (Fig. 17). This suggests that concentration gradients diminish downward from 400 to 500 ft bls approaching the valley (and plume?) axis (Fig. 17). Contaminant concentrations at depths shallower than 200 ft bls are not characterized because these intervals are cased off.

DISCUSSION

The hydrogeological framework of fractured gneiss and granite in this area includes fractures associated with compositional layering, brittle jointing and tectonic shearing of bedrock. The densest concentration of fracture intersections follows the trend of regional strike and plunge gently northeast (Fig. 3). Therefore, structural intersection of layering fractures with subparallel, tectonic shear fractures probably results in pronounced horizontal conductivity in deep bedrock oriented along regional strike. However, ground-water transport in the shallow subsurface (~above 50 ft bls) presumably follows local topographic gradients resulting form the pronounced weathering and ‘openess’ of tectonic fractures (as noted for Site 1) at shallow depths. It is important to note again that most of the conductive brittle fractures dip gently-to-moderately northwest, so that DNAPLS can migrate through shallow- to-intermediate depths in directions other than that of layering dip under natural flow conditions.

The eastern boundary of the contaminant plume near Site 2, at the time of the June 2004 sampling event, is formed by a topographic ridge along the southeast of the valley (Fig. 17). A cross-strike (northwest-southeast trending) topographic divide also separates the proposed housing development and the adjacent landfill into separate surface-water basins draining to the northeast and southwest respectively. The development is therefore situated at the head of the northeast drainage. Migration of the plume from the landfill area into the valley to the northeast would be facilitated by the trend of geological structures. But migration past the crests of the ridges flanking the valley to the northwest and southeast probably would be minimal, so that the plume would be chiefly situated along the axis of the valley. Ground water probably is recharged from the two flanking ridges into the valley where it flows under natural hydraulic gradients northeastward to local surface discharges mapped just beyond the limits of the development. Natural, upward-directed cross flows in the valley, and in the test wells, may promote natural remediation of the VOC plume in the bedrock aquifer by

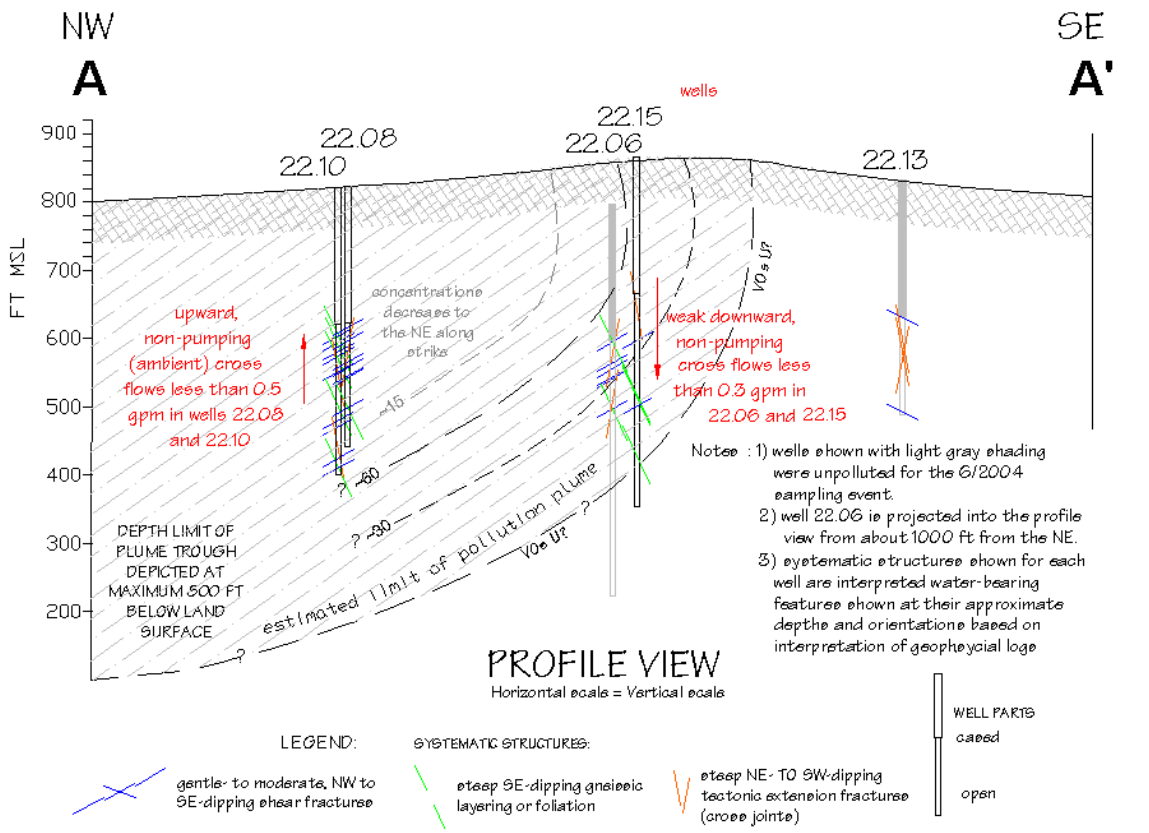

Figure 17. Schematic profile of the hydrogeologic framework of fractured bedrock at Site 2. Location of cross-section shown on figure 3.

bringing deep pollutants upward into contact with conductive fracture planes filled with iron-bearing minerals. Natural, upward-directed cross flows in the test wells facilitate rapid transport of pollutants out of bedrock to more shallow levels close to surface discharge over time. Contamination of the bedrock aquifer probably extends below the 500-ft depth of the OPTV investigation. The vertical extent of the pollution plume is estimated to extend to about 700-ft bls based on the distribution of contaminated wells, interpolated contaminant concentration gradients, and the distribution of 'altered' fractures noted above. However, the lower limit of the plume is queried due to uncertainty (Fig. 17).

REFERENCES

Drake, A. A., Jr., Volkert, R. A., Monteverde, D. H., Herman, G. C., Houghton, H. F., Parker, R. A., and Dalton, R. F., 1996, Bedrock geological map of northern New Jersey: U.S. Geological Survey Miscellaneous Investigation Series Map I-2540-A, scale 1:100,000, 2 sheets.

EnviroMetal Technologies, Inc., 1998, Metal-enhanced dechlorination of volatile organic compounds using an in-situ reactive iron wall, Innovative Technology Evaluation Report, National Risk Management Research Laboratory, Office of Research and Development, U.S. Environmental Protection Agency, EPA/540/R-98/501, 104 p.

Gallagher, R.A. and Volkert, R.A., 1990, Lithologic control of contaminant distribution in ground-water from Middle Proterozoic rocks: An example from the New Jersey highlands: Geological Society of America Abstracts with Programs, Vol. 22, No. 2, p. 19.

Herman, G. C., 2005, Joints and veins in the Newark basin, New Jersey, in regional tectonic perspective: *in* Gates, A. E., ed., Newark Basin – View from the 21st Century, 22nd Annual Meeting of the Geological Association of New Jersey, College of New Jersey, Ewing, New Jersey, p. 75-116; http://www.ganj.org/2005/NB_joints_veins.pdf.

Herman, G.C. 2006, Field Tests Using a Heat-Pulse Flow Meter to Determine it's Accuracy for Flow Measurements in Bedrock Wells, New Jersey Geological Survey Technical Memorandum TM 06-1, 8 p.

Herman, G. C., Monteverde, D. H., Schlische, R. W., and Pitcher, D. M., 1997, Foreland crustal structure of the New York recess, northeastern United States: Geological Society of America Bulletin, v. 109, no. 8, p. 955-977.

Volkert, R.A., 1989, Provisional geologic map of the Proterozoic and Lower Paleozoic rocks of the Califon Quadrangle, Hunterdon and Morris Counties, New Jersey: NJ Geological Survey Geological Map Series Map 89-3, Scale 1:24,0000.